



**The Owl Sensor: a 'Fragile' DNA Nanostructure for Analysis of Single Nucleotide Variations**

Journal:	<i>Nanoscale</i>
Manuscript ID	NR-ART-02-2018-001107.R1
Article Type:	Paper
Date Submitted by the Author:	15-Apr-2018
Complete List of Authors:	Karadeema, Rebekah; University of Central Florida, Chemistry Department Stancescu, Maria; University of Central Florida, Chemistry Steidl, Tyler; University of Central Florida, Chemistry Bertot, Sophia; University of Central Florida, Chemistry Kolpashchikov, Dmitry; University of Central Florida, Chemistry

# The Owl Sensor: a 'Fragile' DNA Nanostructure for Analysis of Single Nucleotide Variations

Rebekah J. Karadeema,<sup>†</sup>\* Maria Stancescu,<sup>†</sup> Tyler P. Steidl,<sup>††</sup> Sophia C. Bertot,<sup>‡†</sup> and Dmitry M. Kolpashchikov<sup>†‡¶\*\*</sup>

<sup>†</sup>Chemistry Department, University of Central Florida, Orlando, FL 32816, USA

<sup>‡</sup>Current address: Department of Chemistry, The Scripps Research Institute, 10550 North Torrey Pines Road, La Jolla, California 92037, United States

<sup>¶</sup>Burnett School of Biomedical Sciences, University of Central Florida, Orlando, 32816, Florida, USA

<sup>¶¶</sup>National Center for Forensic Science and Burnett School of Biomedical Sciences, University of Central Florida, Orlando, Florida, 32816, United States

<sup>\*\*</sup>ITMO University, Laboratory of Solution Chemistry of Advanced Materials and Technologies, Lomonosova St. 9, 191002, St. Petersburg, Russian Federation

E-mail: rebekah@scripps.edu; dmitry.kolpashchikov@ucf.edu

KEYWORDS: DNA nanotechnology • DNA crossover tile • SNP analysis • fluorescent sensor • molecular beacon probe.

---

**ABSTRACT:** Analysis of single nucleotide variations (SNVs) in DNA and RNA sequences is instrumental in healthcare for detection of genetic and infectious diseases and drug-resistant pathogens. Here we took advantage of developments in DNA nanotechnology to design a hybridization sensor, named the 'Owl Sensors', which produce a fluorescent signal only in complex with a fully complementary DNA or RNA analytes. The novelty of Owl Sensor operation is that selectivity of analyte recognition is, at least in part, determined by the structural rigidity and stability of the entire DNA nanostructure rather than exclusively by the stability of the analyte-probe duplex, as is the case for conventional hybridization probes. Using two DNA and two RNA analytes we demonstrated that Owl Sensors differentiate SNVs in a wide temperature range of 5°C-32°C, a performance unachievable by conventional hybridization probes including molecular beacon probe. Owl Sensor's reliably detects cognate analytes even in the presence of 100 times excess of single base mismatched sequences. The approach, therefore, promises to add to the toolbox for diagnosis of SNVs at ambient temperatures.

---

The diagnosis and appropriate treatment of human genetic disorders and infectious diseases rely on the analysis of single nucleotide (nt) variations (SNVs), which include substitutions, insertions, and deletions.<sup>1</sup> Hybridization probes traditionally used for SNV analysis bind a fragment of DNA or RNA containing an SNV site and form a complex, which has greater stability if fully complementary, i.e. all Watson-Crick base pairs are formed between the probe and the analyte, than if a single mispairing is present.<sup>2</sup> Upon subjection of the complex to increasing temperatures the fully matched hybrid decomposes (melts) at higher temperatures than the mismatched complex.<sup>3</sup> This technique enables differentiation of SNVs at high temperatures (>40°C), but only over narrow temperature intervals. The variations of hybridization probes developed so far include peptide nucleic acids (PNAs),<sup>4</sup> locked nucleic acids (LNAs),<sup>5</sup> molecular beacon (MB) probes,<sup>6</sup> and binary probes.<sup>7</sup> All probes rely on this same idea for SNV analysis: the difference in the Gibbs energies between matched and mismatched complexes, which has constant and limited value.<sup>8</sup> For example, if the probe binds a 10-nt segment (which is close to the

shortest possible in practice), a single base mispairing will destabilize the complex by only ~10% on average. While increasing the length of the recognized fragment provides greater affinity and sensitivity, a mispairing then contributes a proportionally lower destabilization effect, leading to even poorer differentiation. Balancing probe affinity and selectivity is a fundamental limitation of the conventional hybridization probes.<sup>8</sup> Therefore, despite many years of efforts, SNV analysis by hybridization probes remains challenging, especially at temperatures below 40°C.<sup>7-9</sup> On the other hand, enzymes recognize SNVs at ambient temperatures, presumably due to their more sophisticated recognition strategy.<sup>10</sup> We hypothesized that enzyme-free DNA probes that, along with the base pairing, use additional principles of target recognition would enable high selectivity of SNV recognition even at ambient temperatures. One implementation of the idea is multicomponent X sensors (see below),<sup>11</sup> which differentiates mismatches at ambient temperature.

In this work, we were inspired by the engineering concept that recognizes that a small and localized failure in an 'imper-

fectly' designed system is likely to result in a structure's collapse. For example, a stable bridge, but not the one with a structural defect, can absorb stress on its support system.<sup>12</sup> Keeping in mind that a rigid object fails more easily than a ductile/flexible one,<sup>13</sup> we took advantage of DNA nanotechnology<sup>14</sup> and designed a DNA sensor that forms a rigid and structurally imperfect complex when binds to a complementary analyte. A single base mismatch serves the role of 'stress' and causes the collapse of the entire fluorescent structure, allowing the sensor to effectively differentiate between fully complementary and mismatched analytes.

The Owl Sensor consists of two DNA adaptor strands  $R_x$  and  $P_y$  and a universal molecular beacon (UMB) probe. UMB probe does not directly binds analytic and therefore can be used for analysis of any sequence giving that adaptor stands are adjusted accordingly.<sup>15</sup> The central portions of the adaptor strands are complementary to an analyte and are thus called analyte-binding domains, while the 4- to 5-nt long 3' and 5' terminal sequences are complementary to UMB. The adaptor strands are named  $R_x$  and  $P_y$  (Figure 1a), where x and y stand for the number of nts in the analyte-binding domains. In the presence of a specific analyte,  $R_x$  and  $P_y$  bind to both UMB and the analyte thus forming a 4-stranded fluorescent structure, which, when drawn, resembles owl eyes, suggesting the name of the structure and the sensor. The structure contains a DNA 4-way junction (crossover) motif commonly used in DNA and RNA nanotechnology.<sup>16</sup>

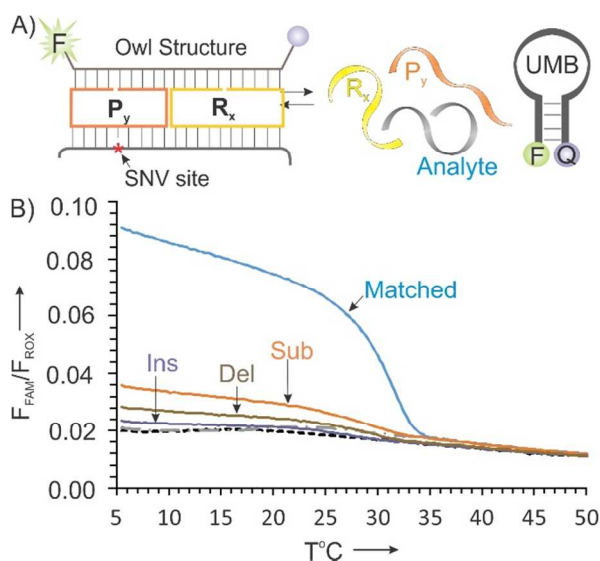


**Figure 1.** Design and performance of Owl Sensor. A) The adaptor strands  $R_x$  and  $P_y$  reversibly hybridize to the analyte and the universal molecular beacon (UMB) probe, forming a fluorescent Owl Structure (see Figure S1 for more details). B) Melting curves for  $R_{10}/P_9$  Owl Sensor ( $R_{10}$ : 5'-TAT TGA GTG GCC CAT CGA TC,  $P_9$ : 5'-TAA CTG TTG TGT CTA TGT; and **UMB1**, 5'-/FAM/-CGC GTT AAC ATA CAA TAG ATC GCG-/BHQ1/) in the presence of fully matched **InhC** (5'-GCG GCA TGG GTA TGG GCC ACT GAC ACA ACA CAA GGA C) or SNV-containing analytes: substitution (Sub), deletion (Del) or insertion (Ins) (see Table S1 for full sequences). Grey dotted-dashed line: no analyte control; black dashed line: **UMB1** only. The samples contained 50 mM Tris-HCl, pH 7.4, 50 mM MgCl<sub>2</sub>, and 0.1% Tween-20 with 50 nM **UMB1**, 50 nM ROX, 150 nM **R10**, 200 nM **P9**, and 100 nM analytes. ROX dye was used as an internal control for normalization of fluorescence from different samples (see SI for details). The experimental data are average of 3 experiments.

As a model analyte, we used a fragment of a gene which codes for enoyl-acyl carrier protein reductase (*inhA*), a target

for the antibiotic isoniazid, which is a common treatment of *Mycobacterium tuberculosis* (*Mtb*) infection.<sup>17</sup> SNVs in this gene are known to impart *Mtb* resistance to isoniazid.<sup>17</sup> The analyte named **InhC** was fully matched to the sensor, while **InhT** contained a G-T mispairing, which is known to be the least destabilizing and, therefore, the most challenging to detect mismatch in DNA.<sup>18</sup> We also designed an analyte with a one-nucleotide deletion, **Inh\_del**, and an analyte with a one-nucleotide insertion, **Inh\_ins** (Table S1), mutations not seen in *Mtb*, but allowing for the versatility of the sensor to be demonstrated. The analytes folded in a relatively unstable secondary structure under the assay conditions (Figure S1). The sequence of the **UMB1** probe (see Figure 1 legend) was optimized by us earlier.<sup>15</sup> In this study, we demonstrate that the Owl Sensor enables differentiation of fully matched analytes from SNV-containing analytes in a broad temperature range that includes ambient temperatures. Furthermore, we aimed to show that this property, at least in part, can be attributed to the rigidity of the Owl Structure.

The Owl Structure is more rigid than dsDNA formed in the case of conventional probes because (i) DNA crossover tiles (even with free ends) are known to be more rigid than dsDNA;<sup>16</sup> and (ii) the ends of the P and R strands are fixed, both by hybridization to **UMB1** and by stacking interactions of the both 3' and 5' terminal base pairs in each strand. To the best of our knowledge, this last feature is absent in the designs of all other hybridization probes, where the location of the ends of the probe is independent on the DNA helical path. Therefore, the length of the analyte-binding fragment of  $R_x$  and  $P_y$  should correspond to a full helical turn of B DNA (~10 nts) to provide the greatest stability of the Owl Structure.

Indeed, when different lengths of  $R_x$  with  $P_{10}$  were tested, we found that  $R_{10}/P_{10}$  produced the highest melting temperature, an indication of complex stability (compare Figure 1 with S2). However, as expected, the stable  $R_{10}/P_{10}$  complex was able to tolerate an SNV and thus produced nearly the same signal in the presence of the mismatched **InhT** as with the fully matched **InhC** (Figure S2C). This proves our hypothesis that 'perfectly' designed DNA nanostructures (Owl complex formed by  $R_{10}$  and  $P_{10}$ ) are able to tolerate stress in the form of base mispairing. For the Owl Sensor to collapse in the presence of a mismatch, 'imperfect' designs were explored, in which the lengths of analyte-binding fragments were changed from a perfect 10 to imperfect 12, 11, 9 or 8 nts (Figures 1, S2, and S3). We found that  $R_{10}/P_9$  allows for complex formation from 5 to about 34°C with the correct analyte, while SNV-containing analytes resulted in little or no signal above the background in this temperature interval (Figure 1B). This result supports our assumption that the  $R_{10}/P_9$  Owl Sensor cannot withstand additional stress introduced by SNVs due to the strain in the structure induced by 'imperfect helicity' (Figure 1a).  $R_{10}/P_8$  produced no signal above the background in the presence of either analyte (Figure S3) due to insufficient stability of the Owl Structure.

We then compared SNV differentiation ability of the  $R_{10}/P_9$  Sensor with Linear, MB probes and X sensor, which were designed to differentiate SNVs according to the previously developed strategies<sup>5,6,11</sup> (Figure 2A). Figure 2B demonstrates the ratios of fluorescent signal in the presence of fully matched **InhC** to that of single base mismatched **InhT**. We assumed that the SNV was differentiated if the signal of the matched analyte ( $F_m$ ) divided by that of the mismatched

analyte ( $F_{mm}$ ) was greater than 1.5, a parameter named  $\Delta T_{1.5}$ .<sup>11d</sup> Based on this criterion, the  $R_{10}/P_9$  Owl Sensor differentiated the SNV between 5 and 32.4°C ( $\Delta T_{1.5} = 27.4^\circ\text{C}$ ), an interval significantly greater than that for the Linear probe ( $\Delta T_{1.5} = 14.8^\circ\text{C}$ ), MB probe ( $\Delta T_{1.5} = 15.6^\circ\text{C}$ ), and X sensor ( $\Delta T_{1.5} = 17.9^\circ\text{C}$ ). Similar results were obtained for the deletion- and insertion-containing analytes (Figure S6), as well as for the  $R_{10}/P_9$  Owl Sensor specific to the **InhT** analyte (Figure S7). Importantly, the Linear and MB probes differentiated analytes at temperatures above physiological values ( $> 45^\circ\text{C}$  Figure 2B), which is common for conventional probes.<sup>5,6</sup> Therefore, the Owl Sensor has two practical advantages over the traditional hybridization probes: it enables (i) broadening the temperature differentiation range, and (ii) shifting its differentiation interval to lower (ambient) temperatures. The limit of detection (LOD) of the Owl Sensor was found to be 4.9 nM, which was not significantly affected by the presence of 100 times excess of the single base mismatched analyte (Figure S7). This LOD is comparable with that of MB probes.<sup>6b</sup>

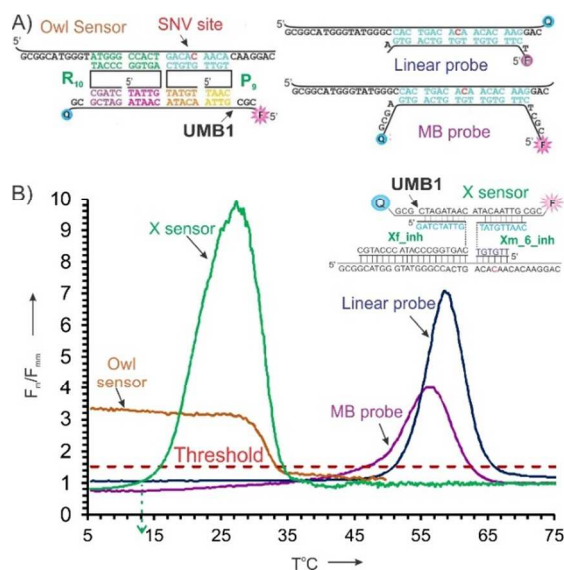


**Figure 2.** SNV differentiation by various hybridization probes. A) Owl Sensor  $R_{10}/P_9$ , Linear probe, MB probe, and the X sensor in complex with analyte **inhC/inhC<sub>Q</sub>**. The red 'C' indicates the location of the SNV site. B) Differentiation ability ( $F_m/F_{mm}$ ) of the linear probe (blue line), the MB probe (purple line), X sensor (magenta line) and the Owl Sensor (green line) as a function of temperature.  $F_m/F_{mm}$  is defined as a ratio of fluorescence intensities produced by each probe in the presence of fully matched analyte ( $F_m$ ) **inhC** to that of mismatched **inhT** analyte ( $F_{mm}$ ) after subtraction of the background. **inhT** analyte contained a C>T substitution with respect to **inhC** analyte. Unless otherwise specified, the P strand of the Owl Sensor was specific to the **inhC** version of the analyte. The threshold of  $F_m/F_{mm} \sim 1.5$  is indicated by the red dotted line. The original fluorescent data used for the plot are shown in Figures 1B and S4. The experimental data are average of 3 experiments.

The remarkably improved SNV differentiation ability of  $R_{10}/P_9$  in comparison with the  $R_{10}/P_{10}$  sensor could be explained by both the reduced stability of the analyte-P9 in comparison with analyte-P10 complex, as is the case for the conventional probes. Alternatively, the instability of the Owl Structure as a whole due to the 'imperfect' design could be the main contributor to its differentiation ability. If the latter is true, addition of structural flexibility to the Owl Structure should jeopardize this extraordinary SNV differentiation ability.

**Table 1:** Quantitative assessment of the stability and differentiation ability ( $\Delta T_{1.5}$ ) of the  $R_{10}/P_9$  Owl Sensor with and without TEG linkers.

DNA strand combinations <sup>a</sup>		$T_m$ , °C	$\Delta T_{1.5}$ , °C		
R	P	InhC	InhT	Inh-Del	Inh-Ins
10	9	31.6	27.6	27.9	27.6
10	9_A	31.5	27.8	27.9	27.8
10	9_o-TEG	31.3	28.0	28.3	27.6
10	9_i-TEG	23.9	20.0	20.8	0.0
10	9_TEG_D	23.7	0.0	0.0	0.0
10_o-TEG	9	26.2	23.1	23.4	11.9
10_TEG_D	9	15.6	8.2	10.5	0.0
10_i-TEG	9	19.0	12.4	13.6	0.0
10_o-TEG	9_o-TEG	25.5	18.2	19.9	0.0
10_i-TEG	9_i-TEG	27.8	24.0	24.0	0.0
10_TEG_D	9_TEG_D	23.8	19.4	19.4	18.2

<sup>a</sup> $T_m$  is a melting temperature determined from the data presented in Figs. 1B 2B, S11, S12, and S13;  $\Delta T_{1.5}$  (see explanation of Figure 2 legend).

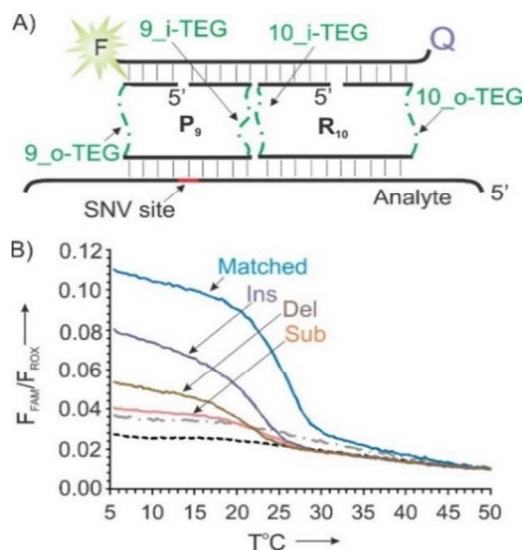


**Figure 3.** Introduction of flexible triethylene glycol (TEG) linkers reduced SNV-differentiation ability of Owl Sensors. A) Location of TEG linkers in the Owl Structure (green). B) Fluorescent response of  $R_{10-oTEG}/P_9$  sensor in the presence of matched **InhC**, or SNV-containing **inh<sub>T</sub>**, **inh<sub>ins</sub>** and **inh<sub>del</sub>**. Grey dotted-dashed line: no analyte control; black dashed line: **UMB1** only. The experimental conditions were as described in Figure 1B legend. The experimental data are average of 3 experiments.

To test this hypothesis, we added flexible triethylene glycol (TEG) linkers between the analyte- and MB-binding arms at the strand crossover points (Figure 3A). PEG linkers connecting two DNA fragments are known to increase the flexibility of DNA constructs.<sup>19</sup> The Owl strands containing linkers had received the following labels: outside junction (o-TEG), inside junction (i-TEG), or to both junctions (TEG\_D) (Figure 3A). TEG-containing Owl Sensors were subjected to the melt curve procedure to determine the effect of their flexibility on the  $T_m$  and  $\Delta T_{1.5}$ . Overall, the SNV differentiation ability of the TEG-containing sensors was significantly reduced:  $\Delta T_{1.5}$  dropped from 27.4°C from  $R_{10}/P_9$  Sensor to as low as 0 for some PEGylated constructs (Table 1). A single TEG linker in the  $R_{10}$  strand resulted in poor differentiation of insertion (Ins) and deletion (Del) SNVs (Figure 3B) in comparison to the linker-free  $R_{10}/P_9$  (Figure 1B). This result suggests that the rigidity of the entire Owl Structure (not only the length of  $P_9$ -analyte complex) is important for SNV differentiation. Interesting, when TEG-containing strands were used, a significant signal with **Inh** analyte was observed, indicating that a flexible system tends to accommodate an extra nucleotide in the analyte strand (Figure S9-11).

Earlier we demonstrated the ability of X sensor to differentiate SNV containing analytes in the temperature interval 5–40°C due to the multistage recognition of the target with the limiting stage requiring the same activation energy for matched and mismatched analytes, which leads to the effect termed ‘kinetic inversion’.<sup>11d</sup> It has been well established that a linear or MB probe equilibrates with a mismatched faster than with a fully matched analytes.<sup>20,11d</sup> Thus achieving equilibrium conditions was considered essential to achieving best SNV differentiation. The ‘kinetic inversion’ effect enables the opposite: faster equilibration of a complex with fully matched nucleic acids, which results in excellent SNV differentiation earlier in the hybridization reaction. For hybridization of the X sensor, we observed the ‘kinetic inversion’ effect in this study. Indeed, the fluorescence of the X sensor in the presence of **Inh\_C** achieved plateau given ~200 s for equilibration, while longer time of ~600 s required for equilibration with mismatched **Inh\_T** (Figure 4, orange lines). It should be noted, that with **Inh** analytes the ‘kinetic inversion’ effect was less pronounced than with analytes used previously,<sup>11d</sup> presumably due to the difference in the stability of analyte secondary structures (a detailed investigation of this difference is in progress). However, we did not observe the ‘kinetic inversion’ effect for Owl sensor: the reaction mixture with mismatched **Inh\_T** reached plateau faster (in about 600 s) than fully matched **Inh\_C** (no signal stabilization even after 1800 s; Figure 4, green lines). We conclude, therefore, that Owl sensor utilizes different SNV differentiation strategy than X sensor, a phenomenon that may become practically important. Indeed, the X sensor, designed according to the previously established rules, failed to differentiate **Inh\_C** from **Inh\_T** at temperatures below 15°C (Figure S11). Therefore, if a differentiation of SNV in analytes with unstable secondary structures needs to be achieved at temperatures below 15°C, the Owl Sensor design should be utilized.

Further we explored the ability of Owl Sensor to analyze RNA sequences. RNA-DNA hybrids typically adopt an A DNA-like conformation with 11.1 bp per helical turn (not 10.4 bp/turn as it is for B DNA). We investigated the performance of a series of Owl Sensors with the RNA analogs of **InhC** and **InhT** analytes (Figure S12, S13). It was found that  $R_{11}/P_9$  performed best (differentiation from 5 to 25.1°C), while  $R_{10}/P_9$  failed to produce a significant signal. This proves that optimum helicity in the R strand is needed for sensing. Owl Sensor, therefore, is applicable

for highly selective analysis of RNA sequences with slight modification of thus suitable for analysis of DNA sequences.

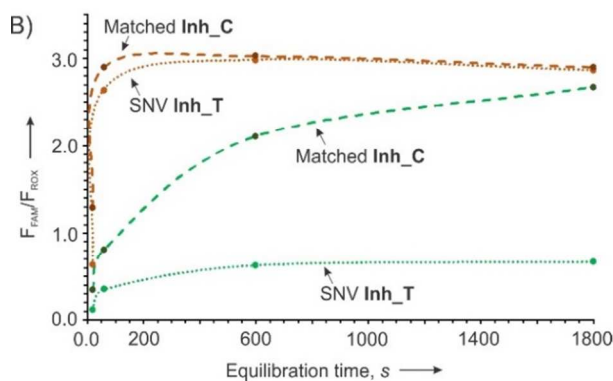


**Figure 4.** Fluorescence of probe-analyte complexes at different rates of the cooling-heating cycle. The fluorescent signal for the equilibration time of 20, 60, 600 or 1800 s/1°C observed for the X sensor-analyte (orange lines) and  $R_{10}/P_9$  Owl Sensor (green lines) at 10°C. In the presence of fully matched **Inh\_C** (dashed lines) or single base mismatched **Inh\_T** (dotted lines). The experimental data are average of 3 experiments.

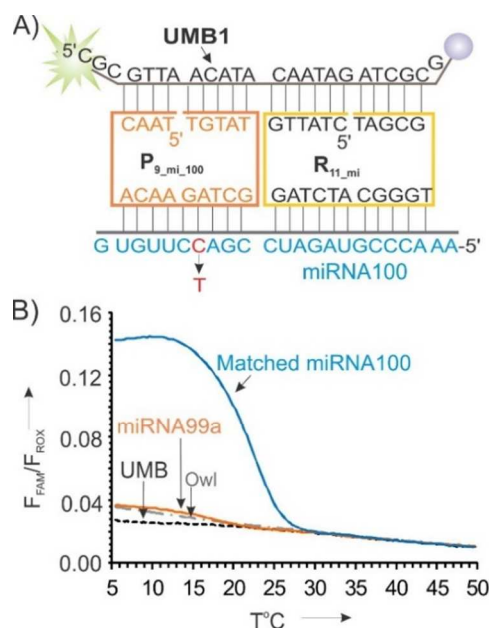


**Figure 5.**  $R_{11}/P_9$  Owl Sensor differentiates single base mismatch in RNA analytes. A)  $R_{11\_mi}/P_{9\_mi\_100}$  sensor in complex with fully matched **miRNA100**. Red letter indicates the SNV position. B) Melting curves for  $R_{11\_mi}/P_{9\_mi\_100}$  complexes with matched **miRNA100** (blue) and single base mismatched **miRNA99a** (orange) analytes. The samples contained 50 mM Tris-HCl, pH 7.4, 10 mM  $MgCl_2$ , and 0.1% Tween-20 with 50 nM **UMB1**, 50 nM ROX, 150 nM  $R_{11\_mi}$ , 200 nM  $P_{9\_mi\_100}$ , and 100 nM analytes. ROX dye was used as an internal control for normalization of fluorescence from different samples (see SI for details). The experimental data are average of 3 experiments.

To prove the general applicability of the Owl Sensor design, we used another pair of arbitrarily chosen analytes: miRNA99a and miRNA100, which differ by a single nt (Table S1, Figure S14,15). Altered expression of these miRNAs has been found in various cancers, including breast cancer.<sup>21</sup> Owl Sensors specific to both RNA and DNA (miDNA99a and miDNA100) versions of the target were designed and tested. As is the case with **Inh**-related analytes,  $R_{10mi}$  was the best for DNA analytes while  $R_{11mi}$  per-

formed best for RNA analytes (Figures S16,17). We also observed high selectivity of SNV recognition under ambient temperatures (Figures S17). The corresponding **miRNA100** was differentiated with high selectivity from **miRNA99a** using **R<sub>11\_mi</sub>/P<sub>9\_mi\_100</sub>** sensor (Figure 5), but not sensors with **R<sub>10\_mi</sub>** or **R<sub>12\_mi</sub>** strands (Figure S18,19). These results suggest general applicability of the Owl Sensor design for analysis of potentially any DNA or RNA sequence. We also investigated the sensor's performance in access amount of unrelated biological RNA. It was found that presence of 2.5 mg/L or 25 mg/L yeast RNA does not significantly affect the performance of the Owl Sensor (Figure S20). This data further highlights the high selectivity of the developed approach as well as robustness of Owl Sensor performance in the presence of bulk amounts of biological molecules.

Traditional design of SNV-specific hybridization probes is a time-consuming. Even if perfectly designed and under optimal hybridization conditions, such sensors have limited SNV selectivity, especially at practically important ambient temperatures. Here we applied of a new concept of analyte recognition, in which a hybridization sensor uses an analyte as a scaffold to build a rigid and fragile nanostructure that is too unstable if an SNV is present. The design procedure is as follows: (i) always use **UMB1** (5'-/FAM/-CGC GTT AAC ATA CAA TAG ATC GCG-/BHQ1/) as a fluorescent reporter; (ii) always use **UMB1**-binding arms for strands P and R as shown in Figure 2 and 5 for DNA and RNA analytes, respectively; (iii) SNP site should be located in the middle position of P strand-binding region; (iv) analyte binding arm of strand R should hybridize adjacent to the hybridization site of strand P and should be 10 and 11 nucleotides for analysis of DNA and RNA analytes, respectively. Therefore, unlike conventional hybridization-based sensors, these design promises to eliminate the need for adjusting the probe lengths or the hybridization conditions to achieve near-perfect selectivity. The new sensor selectively binds only fully complementary DNA and RNA and discriminates against single base substitutions, deletions, and insertions in a broad temperature range even in the presence of random RNA or excess amount of single base-mismatched analyte. For two different analyte sequences, it was shown that 10 and 9 nts for the R and P strands, respectively, were ideal for DNA-targeting sensors, while 11 and 9 nts for the R and P strands, respectively, worked best for RNA targeting. Follow up studies are in progress for further verification of general applicability of the Owl Sensor for DNA and RNA analysis. Importantly, **UMB1** does not hybridize directly to the analyte in the Owl complex and, therefore, can be used universally for any analyte, provided that strands P and R are tailored for targeted sequences. The Owl Sensor, therefore, promises to simplify design and optimization of hybridization assays and will contribute to low cost, ambient temperature analysis of DNA and RNA.

## ASSOCIATED CONTENT

**Supporting Information.** Supporting Information contains details of experimental procedures, list of all DNA and RNA sequences used in this study as well as the experimental data supporting the conclusions made in this study.

## AUTHOR INFORMATION

### Corresponding Author

\*Rebekah J. Karadeema E-mail: rebekah@scripps.edu and  
\*Dmitry M. Kolpashchikov Dmitry.Kolpashchikov@ucf.edu.

### Present Addresses

†Department of Chemistry, The Scripps Research Institute, 10550 North Torrey Pines Road, La Jolla, California 92037, United States.

## Author Contributions

The manuscript was written through contributions of all authors. All authors have given approval to the final version of the manuscript.

## Funding Sources

The project was supported by NSF CCF 1423219 and NSF CBET 1706802. D. M. K. was supported by the ITMO University Fellowship and Professorship Program.

## Notes

Any additional relevant notes should be placed here.

## ACKNOWLEDGMENT

DMK is grateful to Dr. Yulia V. Gerasimova for helpful discussion and help in manuscript preparation.

## ABBREVIATIONS

UMB, universal molecular beacon; nt, nucleotide; SNV, single nucleotide variations; MB, molecular beacon; PNAs, peptide nucleic acids; LNAs, locked nucleic acids; *Mtb*, *Mycobacterium tuberculosis*; LOD, limit of detection; F<sub>m</sub>, Fluorescence of matched analyte; F<sub>mm</sub>, Fluorescence of mismatched analyte; T<sub>m</sub>, melting temperature; TEG, triethylene glycol.

## REFERENCES

- (1) (a) Aphasizheva, I.; Aphasizhev, R. *Trends Parasitol.* **2016**, *32*, 144-156. (b) Makova, K. D.; Hardison, R. C. *Nat. Rev. Genet.* **2015**, *16*, 213-323; (c) Yu, C.; Baune, B. T.; Licinio, J.; Wong, M. L. *Psychiatry Res.* **2017**, *252*, 75-79.
- (2) (a) Marras, S. A.; Tyagi, S.; Kramer, F. R. *Clin. Chim. Acta.* **2006**, *363*, 48-60; (b) Boutorine, A. S.; Novopashina, D. S.; Krasheninina, O. A.; Nozeret, K.; Venyaminova, A. G. *Molecules* **2013**, *18*, 15357-15397; (c) Guo, J.; Ju, J.; Turro, N. *Analytical & Bioanalytical Chemistry* **2012**, *402*, 3115. (d) Junager, N. P.; Kongsted, J.; Astakhova, K. *Sensors (Basel)* **2016**, *16*, pii: E1173.
- (3) (a) Erali, M.; Voelkerding, K. V.; Wittwer, C. T. *Exp Mol Pathol.* **2008**, *85*, 50-58. (b) Fontenete, S.; Guimarães, N.; Wengel, J.; Azevedo, N. F. *Crit. Rev. Biotechnol.* **2016**, *36*, 566-577; (c) Tong, S. Y.; Giffard, P. M. *J. Clin. Microbiol.* **2012**, *50*, 3418-3421.
- (4) Zhang, N.; Appella, D. H. *J. Infect. Dis.* **2010**, *201*, S42-5. (b) Liu, Q.; Wang, J.; Boyd, B. *J. Talanta* **2015**, *136*, 114-127; (c) Lee, J.; Park, I. S.; Jung, E.; Lee, Y.; Min, D. H. *Biosens Bioelectron.* **2014**, *62*, 140-144; (d) Smolina, I. V.; Frank-Kamenetskii, M. D. *Methods Mol Biol.* **2014**, *1050*, 121-130; (e) Sharma, C.; Awasthi, S. K. *Chem. Biol. Drug Des.* **2017**, *89*, 16-37.
- (5) (a) Campbell, M. A.; Wengel, J. *Chem Soc Rev.* **2011**, *40*, 5680-5689. (b) Xi, D.; Shang, J.; Fan, E.; You, J.; Zhang, S.; Wang, H. *Anal. Chem.* **2016**, *88*, 10540-10546; (c) Fontenete, S.; Carvalho, D.; Guimarães, N.; Madureira, P.; Figueiredo, C.; Wengel, J.; Azevedo, N. F. *Appl. Microbiol. Biotechnol.* **2016**, *100*, 5897-5906.
- (6) (a) Tyagi, S.; Kramer, F. R. *Nature Biotechnology* **1996**, *14*, 303-308. (b) Kolpashchikov, D. M. *Scientifica* **2012**, 928783.
- (7) Kolpashchikov, D. M. *Chem. Rev.* **2010**, *110*, 4709-4723.
- (8) (a) Demidov, V. V.; Frank-Kamenetskii, M. D. *Trends Biochem. Sci.* **2004**, *29*, 62-71; (b) SantaLucia Jr, J.; Hicks, D. *Annual Review of Biophysics & Biomol. Structure* **2004**, *33*, 415-440.
- (9) (a) Wegman, D. W.; Ghasemi, F.; Stasheuski, A. S.; Khorshidi, A.; Yang, B. B.; Liu, S. K.; Yousef, G. M.; Krylov, S. N.; *Anal. Chem.* **2016**, *88*, 2472-2477. (b) Urakawa, H.; El Fantroussi, S.; Smidt, H.; Smoot, J. C.; Tribou, E. H.; Kelly, J. J.; Noble, P. A.; Stahl, D. A. *Applied and Environ. Microbiol.* **2003**, *69*, 2848-2856.
- (10) (a) Olivier, M. *Mutat Res.*, **2005**, *573*, 103-110; (b) Drabovich, A. P.; Krylov, S.N. *Anal. Chem.* **2006**, *78*, 2035-2038; (c) Y. V. Gerasimova, D. M. Kolpashchikov, *Chem. Soc. Rev.* **2014**, *43*, 6405-6438; (d) (f) Streat, M.; Detmer, I.; Gaster, J.; Marx, A. *Methods Mol. Biol.*, **2007**, *402*, 317-328.
- (11) (a) Kolpashchikov D. M. *J. Am. Chem. Soc.* **2006**, *128*, 10625-10628; (b) Gerasimova, Y. V.; Kolpashchikov, D. M. *Biosens Bioelectron.* **2013**,

- 41, 386-390; (c) Gerasimova Y. V.; Ballantyne, J.; Kolpashchikov D. M. *Methods Mol. Biol.* **2013**, 1039, 69-80; (d) Stancescu, M.; Fedotova, T.A.; Hooyberghs, J.; Balaeff, A.; Kolpashchikov, D. M. *J. Am. Chem. Soc.* **2016**, 138, 13465-13468.
- (12) Feld, J. Carper, K. L. **1997**, John Wiley & Sons. ISBN 0-471-57477-5.
- (13) Rice, P.; Dutton H. **1995**, Taylor & Francis. p. 33
- (14) (a) Jones, M. R.; Seeman, N. C.; Mirkin, C. A. *Science* **2015**, 347, 1260901; (b) Jaeger, L.; Chworos, A. *Curr. Opin. Struct. Biol.* **2006**, 16, 531-543; (c) Roh, Y. H.; Ruiz, R. C.; Peng, S.; Lee, J. B.; Luo, D. *Chem. Soc. Rev.* **2011**, 40, 5730-5744; (d) Endo, M.; Sugiyama, H. *ChemBiochem* **2009**, 10, 2420-2443.
- (15) Gerasimova, Y. V.; Hayson, A.; Ballantyne, J.; Kolpashchikov, D. M. *ChemBioChem* **2010**, 11, 1762-1768.
- (16) (a) Fu, T.-J.; Seeman, N. C. *Biochemistry* **1993**, 32, 3211-3220; (b) Eichman, B. F.; Vargason, J. M.; Blaine, H. M. M.; Ho, P. S.; *Proc. Natl Acad. Sci. U. S. A.* **2000**, 97, 3971-3976; (c) Kolpashchikov, D. M.; Gerasimova, Y. V.; Khan, M. S. *ChemBiochem* **2011**, 12, 2564-2567; (c) B. Kim, S. Jo, J. Son, J. Kim, M. H. Kim, S. U. Hwang, S. R. Dugasani, B. D. Kim, W. K. Liu, M. K. Kim, S. H. Park, *Nanotechnology* **2014**, 25, 105601. (d) Boulais É.; Sawaya N. P. D.; Veneziano R.; Andreoni A.; Banal, J.L.; Kondo, T.; Mandal, S.; Lin, S.; Schlau-Cohen, G. S.; Woodbury, N. W.; Yan, H.; Aspuru-Guzik, A.; Bathe, M. *Nat. Mater.* **2017**, doi: 10.1038/nmat5033; (e) Stewart, J. M.; Subramanian, H. K. K.; Franco, E. *Nucleic Acids Res.* **2017**, 45, 5449-5457; (f) Stewart, J. M.; Viard, M.; Subramanian, H. K.; Roark, B. K.; Afonin, K. A.; Franco, E. *Nanoscale* **2016**, 8, 17542-17550; (g) Lau, K. L.; Sleiman, H.F. *ACS Nano.* 2016, 10, 6542-6551; (h) Son, J.; Lee, J.; Tandon, A.; Kim, B.; Yoo, S.; Lee, C. W.; Park, S.H. *Nanoscale* 2015, 7, 6492-6497.
- (17) Mdluli, K.; Slayden, R. A.; Zhu, Y.; Ramaswamy, S.; Pan, X.; Mead, D.; Crane, D. D.; Musser, J. M.; Barry, C. E. *Science* **1998**, 280, 1607-1610.
- (18) Allawi, H. T.; SantaLucia, J. Jr. *Biochemistry* **1997**, 36, 10581-10594.
- (19) (a) Pyshnaya I. A., Pyshnyi D. V., Lomzov A. A., Zarytova V. F., Ivanova E. M. *Nucleosides Nucleotides Nucleic Acids.* 2004, 23, 1065-1071; (b) Pyshnyi D. V., Lomzov A. A., Pyshnaya, I.A., Ivanova E. M. *J. Biomol. Struct. Dyn.* **2006**, 23, 567-580.
- (20) (a) Wang, S.; Friedman, A. E.; Kool, E. T. *Biochemistry*, **1995**, 34, 9774-9784; (b) Dai, H.; Meyer, M.; Stepaniants, S.; Ziman, M.; Stoughton, R. *Nucleic Acids Res.*, **2002**, 30, e86; (c) Hooyberghs, J.; Baiesi, M.; Ferrantini, A.; Car-lon, E. *Physical Review E*, **2010**, 81, 012901. (d) Rauzan, B.; McMichael, E.; Cave, R.; Sevcik, L.R.; Ostrosky, K.; Whitman, E.; Stegemann, R.; Sinclair, A.L.; Serra, M. J.; Deckert, A. A. *Biochemistry*, **2013**, 52, 765-772.
- (21) Wu, D.; Zhou, Y.; Pan, H.; Qu, P.; Zhou, J. *Mol. Med. Rep.* **2015** 11, 1469-1475.

SYNOPSIS TOC A deliberately unstable fluorescent DNA nanostructure (Owl Structure) is not formed when a single base mismatch additionally destabilizes it.

---

